Korean J. Chem. Eng., **26**(1), 269-276 (2009)

Brownian diffusion effect on nanometer aerosol classification in electrical mobility spectrometer

Panich Intra*,† and Nakorn Tippayawong**

*College of Integrated Science and Technology, Rajamangala University of Technology Lanna, Chiang Mai 50300, Thailand
**Department of Mechanical Engineering, Faculty of Engineering, Chiang Mai University, Chiang Mai 50200, Thailand
(*Received 27 May 2008 • accepted 26 June 2008*)

Abstract−A multi-channel differential mobility analyzer (MCDMA) or aerosol spectrometer is widely used for classifying and measuring nanometer aerosol particles in the size range from 1 nm to 1 μm because of its better time response than a typical differential mobility analyzer. In the present study, the effect of Brownian diffusion on electrical mobility classification and trajectory of nanometer aerosol particles in an electrical mobility spectrometer developed at Chiang Mai University has been analytically investigated. Th Brownian diffusion of particles inside the spectrometer increased with decreasing particle size and flow rates of aerosol and clean sheath air, and with increasing inner electrode voltage, and also decreased with decreasing operating pressure. The particle trajectories considering Brownian diffusion motion inside the spectrometer were found to be broader than those under no Brownian diffusion. Smaller particles were found to have higher degree of broadening of trajectory than the larger particles. Brownian diffusion effect was found to be significant for particles smaller than 10 nm.

Key words: Brownian Diffusion, DMA, Electrical Mobility, Nano-aerosol

INTRODUCTION

The differential mobility analyzer (DMA) is one of most commonly used devices for classifying and measuring nanometer aerosol particles in the size range from 1 nm to 1 μm in diameter based on their electrical mobility [1]. The most widely used DMA is based on the design developed by Liu and Pui [2] and Knutson and Whitby [3]. Recent developments of the analyzer have resulted in multi-channel DMA (MCDMA) or aerosol spectrometer where a complete size spectrum of nanometer aerosol particles can be obtained in about 1 s or less [4]. A typical DMA is referred to as a single channel instrument, while an MCDMA is an instrument with multi-channel sensing capability. The MCDMA was first designed in the Bradbury laboratory by Yunker [5]. In later works, Tammet et al. [6], Mirme et al. [7], Matisen et al. [8], and Mirme [9] designed and developed an MCDMA in the Tartu University known as an electrical aerosol spectrometer (EAS) and subsequently improved by Tammet et al. [10]. The EAS is able to classify particles in a similar fashion to, but faster than, a typical DMA due to its multi-channel measurement capability. Graskow [11] developed a fast aerosol spectrometer (FAS). His prototype has better time response than the EAS. Biskos et al. [12] later reported the development of a differential mobility spectrometer (DMS), derived from Graskow's concept. Based on similar principle to previously mentioned instruments, Intra and Tippayawong from Chiang Mai University, Thailand, designed, built and tested an electrical mobility spectrometer (EMS) for aerosol size distribution measurement in the size range of approximately 10-1,000 nm [13,14].

Operation and performance of the EMS depend upon aerosol transport under the influence of flow and electric fields. With regards to sizing ultrafine aerosol particles of diameter less than 100 nm such as in Kim's work [15], Brownian diffusion motion becomes important [16]. The history of the Brownian diffusion in DMA dates back to the first half of the 20th century. Brownian diffusion of ions in DMA was first described already by Zeleny [17] and later by Tammet [18]. Further, Stolzenburg [19] and Salm [20] have developed much more detailed mathematical models of the behavior of diffusive particle in DMAs. There are two main reasons for the need to improve understanding of the particle Brownian diffusion: (i) to quantify the resolution of the particle size distribution, and (ii) to quantify the accuracy of the electrical mobility classification and measurement [21]. In the present paper, a simplified analysis of the effect of particle Brownian diffusion on electrical mobility classification and performance of an MCDMA such as the EMS developed at Chiang Mai University was analytically investigated and discussed. A detailed description of the operating principle of the EMS is presented.

DESCRIPTION OF THE EMS

The EMS has one long column, consisting of coaxially cylindrical electrodes. Fig. 1 shows a schematic diagram of the EMS used in this study. Its geometrical configuration is similar to those reported by Graskow [11], Biskos et al. [12], and Intra and Tippayawong [13,14]. The outer chassis is made of a 481 mm long aluminum tube with an internal diameter of 55 mm. The inner electrode is made of a 25 mm in diameter stainless steel rod. Width of the aerosol inlet channel is 2 mm. The inner electrode was polished to an extremely fine surface finish to avoid undesirable electric field effect on particle motion due to non-uniform electric field from small surface scratches and imperfections. It is important to ensure that both flow and electric fields are laminar and uniformly distributed inside the analyzing column. There are two streams: polydisperse aerosol and

†To whom correspondence should be addressed.
E-mail: panich_intra@yahoo.com, panich.intra@hotmail.com

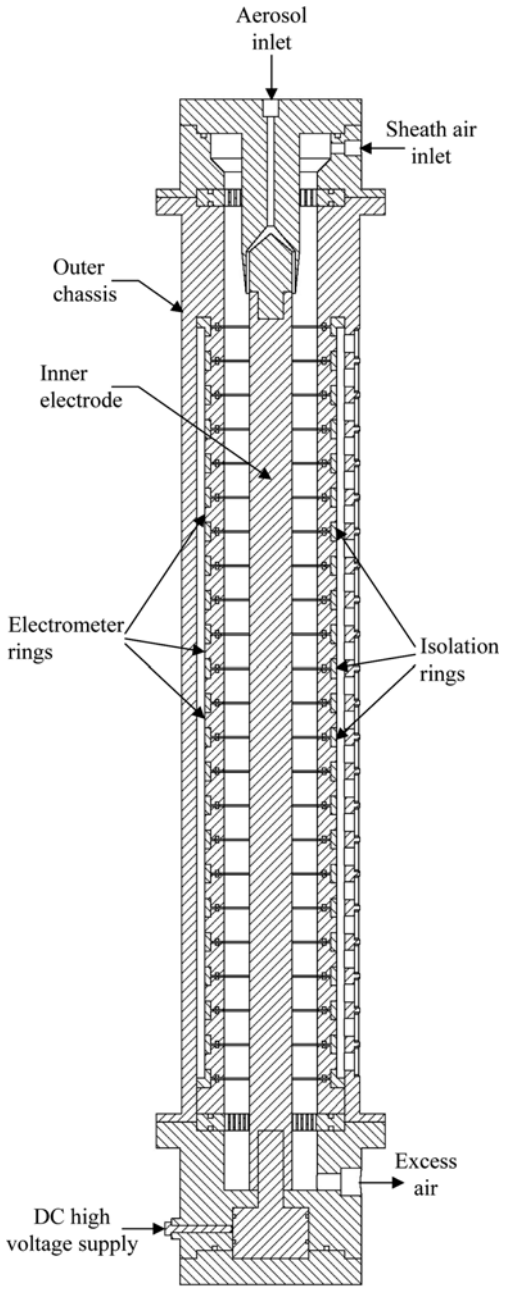

Fig. 1. Schematic diagram of the EMS.

sheath air flows. The inner electrode of the classifier is maintained at a DC high voltage while the outer chassis of the analyzer is grounded. An adjustable DC high voltage power supply is used to maintain this voltage difference, generally in the range between 1.0-5.0 kV. To avoid unintentional charging of the particles within the analyzer, the applied high voltage is maintained at a lower value than the corona onset voltage. The charged particles enter the analyzer column close to the inner electrode by a continuous flow of air and surrounded by a sheath air flow. Since the inner electrode is kept at a high voltage, the charged particles are deflected outward radially. They are collected on a series of electrically isolated electrometer rings positioned at the inner surface of the outer chassis of the analyzer column. Virtual ground potential input of highly sensitive electrometers is connected to these electrometer rings to measure currents corresponding to the number concentration of particles in a given mobility, which is in turn related to the particle size distribution [22]. Resolution of the instrument is determined mainly by the number and width of the electrometer rings. Table 1 shows the width and the position of the electrometer rings along the analyzer column. The 22 electrometer rings used result in the classification of every measured aerosol into 22 mobility ranges. As shown in Table 1, the electrometer rings have a width of 19 mm. The first electrometer ring is located 20 mm downstream the aerosol inlet, while a 1 mm gap is allowed between the electrometer rings for electrical isolation. The size range of particle collected on the electrometer rings can be varied by adjusting the aerosol and sheath air flow rates, the voltage applied to the inner electrode, and the operating pressure.

Table 1. Electrometer ring width and positions along the EMS

Electrometer ring number	Electrometer ring width (mm)	Midpoint location (mm)
1	19	29.5
2	19	49.5
3	19	69.5
4	19	89.5
5	19	109.5
6	19	129.5
7	19	149.5
8	19	169.5
9	19	189.5
10	19	209.5
11	19	229.5
12	19	249.5
13	19	269.5
14	19	289.5
15	19	309.5
16	19	329.5
17	19	349.5
18	19	369.5
19	19	389.5
20	19	409.5
21	19	429.5
22	19	449.5

MODELING OF PARTICLE TRANSPORT INSIDE THE EMS

1. Non-diffusing Particle Trajectory

Fig. 2 shows a schematic diagram of a non-diffusing particle trajectory in the analyzer. The axial motion was influenced by the fluid velocity profile in the axial flow. The radial motion is due to electric force, which is by far greater than other forces. When the particles are introduced into the analyzer column, any charged particle under the influence of an electric field will have an electrical mobility. It is assumed that the flow and electric fields are axisymmetric and steady, the flow in the analyzer is laminar, fully developed and incompressible ($\nabla \cdot u=0$), the space charge effect is negligible ($\nabla \cdot E=0$), and the gravitational and Brownian diffusion effects are negligible. Thus, the total volumetric flow rate, Q_t, through the classifier

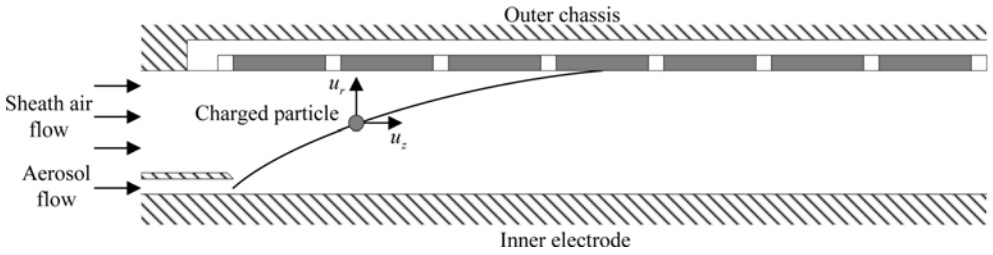

Fig. 2. Schematic diagram of non-diffusing particle trajectory in the EMS.

column is

$$Q_t=Q_{sh}+Q_a \tag{1}$$

where Q_{sh} is the particle free sheath air flow rate and Q_a is the aerosol flow rate. For the particular case of annular geometries where the charged aerosol sample enters the analyzer on an axial flow and the charged particles migrate along the radial direction of electric field, the trajectory of the charged particles within the analyzer can be described by a system of differential equations as

$$\frac{dr}{dt}=u_r+Z_pE_r \tag{2}$$

$$\frac{dz}{dt}=u_z+Z_pE_z \tag{3}$$

where r and z are the radial and axial dimensions of the classifier, u_r and u_z are the radial and axial components of the air flow velocity. Similarly, E_r and E_z are the radial and axial components of the electric field and Z_p is the electrical mobility of particles, and is given by

$$Z_p=\frac{n_p e C_c}{3\pi\mu d_p} \tag{4}$$

where n_p is the number of the charge on the particle, e is the charge of electron (1.6×10^{-19} C), C_c is the Cunningham slip correction factors, μ is the air viscosity and d_p is the particle diameter. The equation above is only valid for particles larger than 3 nm in diameter [23-25]. For pressure other than atmospheric, and assuming no temperature variations, the electrical mobility of the particles is corrected by

$$Z_p=\frac{Z_{patm}P_{atm}}{P} \tag{5}$$

where Z_{patm} is the electrical mobility of the particles at atmospheric pressure, and P_{atm} and P are the reference and operating pressure of the analyzer. When a uniform electric field is established between the two electrodes of the analyzer, the electric field components are given by the following relations

$$E_r=\frac{V}{r\ln(r_2/r_1)} \text{ and } E_z\approx0 \tag{6}$$

where r_1 and r_2 are the radii of the inner and outer electrodes, respectively, and V is the applied voltage. Assuming that the radial velocity component for a laminar annular flow is zero (u_r=0) and combining the above equations, the charged particle trajectories in an inviscid (plug) flow can be described by

$$\frac{dr}{dt}=\frac{Z_pV}{r\ln(r_2/r_1)} \tag{7}$$

$$\frac{dz}{dt}=u_z \tag{8}$$

Using Eqs. (7) and (8), the trajectory of the charged particle is given by

$$\frac{dr}{dz}=\frac{Z_pV}{u_z r\ln(r_2/r_1)} \tag{9}$$

Integrating Eq. (9), the migration paths of the charged particles can be determined as

$$\int_{r_{in}}^{r_2} r dr=\frac{VZ_p}{u_z\ln(r_2/r_1)}\int_0^z dz \tag{10}$$

where r_{in} is the radial position at which the particle enters the analyzer. Assuming that the average flow velocity in the axial direction of the analyzer column is

$$u_{av}=\frac{Q_t}{\pi(r_2^2-r_1^2)} \tag{11}$$

Therefore, the deposition of the charged particles entering the analyzer column at a radial position of r_{in} has a trajectory taking it to an axial position z downstream of the aerosol inlet, which is given in terms of their electrical mobility, the mean flow velocity, and the electric field strength, is

$$z=\frac{Q_t\ln(r_2/r_1)(r_2^2-r_{in}^2)}{2\pi VZ_p(r_2^2-r_1^2)} \tag{12}$$

which can be rearranged in terms of the critical electrical mobility of a particle that is collected on each electrometer rings at distance z downstream of the aerosol inlet as

$$Z_p=\frac{Q_t\ln(r_2/r_1)(r_2^2-r_{in}^2)}{2\pi Vz(r_2^2-r_1^2)} \tag{13}$$

2. Diffusing Particle Trajectory

As a result of random collisions between the aerosol particles and the air molecules, aerosol particles undergo diffusion. Diffusion is reflected in the aerosol particles trajectory as a random perturbation. These perturbations are described by Brownian motion. The trajectory of nanometer-sized particles undergoing Brownian motion in the analyzer column can be described by the equation of convective Brownian diffusion, which is expressed as follows:

$$u(r)\frac{\partial n(r,z)}{\partial r}=D\left\{\frac{\partial^2 n(r,z)}{\partial r^2}+\frac{1}{r}\frac{\partial n(r,z)}{\partial r}+\frac{\partial^2 n(r,z)}{\partial z^2}\right\} -\frac{1}{r}\frac{\partial}{\partial r}\{Z_p rE(r)n(r,z)\} \tag{14}$$

where r and z are the radial and axial positions, u(r) is the axial velocity of gas flow, n is the particle number concentration, and D is the particle diffusion coefficient which is a function of the electrical mobility of particle,

$$D = \frac{kTZ_p}{n_p e} \tag{15}$$

where k is Boltzmann's constant and T is the absolute temperature. For pressure other than atmospheric in the same way as Z_p in Eq. (5), the diffusion coefficient of the particles is given by

$$D = \frac{D_{atm}P_{atm}}{P} \tag{16}$$

where D_{atm} is the diffusion coefficient of the particles at atmospheric pressure. Eq. (14) can be normalized by using three dimensionless parameters in similar fashion to Kousaka et al. [16]

$$\bar{u}(\bar{r}) = \frac{u(r)}{u_{av}}, \tag{17}$$

$$\overline{D} = \frac{Dz}{r_1^2 u_{av}}, \tag{18}$$

$$\overline{E} = \frac{Z_p Vz}{r_1^2 u_{av} \ln(r_2/r_1)}, \tag{19}$$

where $\bar{u}$, $\overline{D}$, and $\overline{E}$ are the normalized gas velocity, diffusivity, and velocity due to electrostatic force, respectively and z is the axial distance. The value of dimensionless parameter $\overline{D}/\overline{E}$ is important in the evaluation of the effect of Brownian diffusion. In the ideal case with no Brownian diffusion motion, the value of dimensionless parameter $\overline{D}/\overline{E}$ becomes zero [16,26]. Brownian motion also causes particles to deviate from their ideal transport paths within the analyzer column, resulting in a diffusion broadening of the mobility range collected on the electrometer ring as shown in Fig. 3. In Brownian diffusion motion, a particle of mobility Z_p arrives at each electrometer ring at a radial position given by a certain probability distribution, which is assumed to be a Gaussian of mean r and standard deviation σ. The mean value of the trajectory end-point distribution is determined by the applied electric field

$$r(t) = \sqrt{r_{in}^2 + \frac{2VZ_p}{\ln(r_2/r_1)}t} \tag{20}$$

where r_{in} is the initial radial position of the particle at time t=0, and t is the mean aerosol residence time between the inlet and electrometer rings. The variance of the trajectory end-point distribution is assumed to be that of a pure Brownian process, and given by

$$\sigma \approx \sqrt{2Dt}, \tag{21}$$

The radial position of particles r_{diff} takes into account the Brownian diffusion motion, a particle which enters the spectrometer at position r_{in} and arrives at electrometer ring at a position $r \pm \sigma$ is given by

$$r_{diff} = r \pm \sigma \tag{22}$$

where r is the radial distance, and σ is the standard deviation of the trajectory end-point distribution for particles. The plus sign indicates the upper limit of the diffusive particle trajectory; the minus sign indicates the lower limit of the diffusive particle trajectory. However, it is not possible to solve these equations explicitly. The most convenient way to overcome this difficulty is to use the average arrival coordinate r in linear form of Eq. (20) [27,28]:

$$r \approx r_{in} + \frac{VZ_p}{r_{in}\ln(r_2/r_1)}t \tag{23}$$

For these particles, the linear form deviates only slightly from the more rigorous Eq. (20). Inserting Eqs. (20), (21) and (23) into Eq. (22) leads to the radial position for diffusive particles.

$$r_{diff}(t) \approx r_{in} + \frac{VZ_p}{r_{in}\ln(r_2/r_1)}t \pm \sqrt{2Dt} \tag{24}$$

Substituting $t = z/u_{av}$ into Eq. (24), the diffusive particle trajectory is

$$r_{diff}(z) \approx r_{in} + \frac{zVZ_p}{u_{av} r_{in}\ln(r_2/r_1)} \pm \sqrt{\frac{2Dz}{u_{av}}} \tag{25}$$

With Eq. (25), the above equation can now be solved explicitly for the diffusive particle trajectory. The diffusing particle trajectory in Eq. (25) can be expressed in terms of the diffusing particle electrical mobility as

$$Z_{p,diff} = \frac{kTr_2^2 \ln^2(r_2/r_1)}{2etV^2}\left[1 + \sqrt{1 + \frac{2eV}{kT\ln(r_2/r_1)}\left(1 - \frac{r_1}{r_2}\right)}\right]^2 \tag{26}$$

This approximation was originally solved by Alonso et al. [28], with maximum relative error less than 1%.

3. Calculation Procedure

An analytical model was developed to investigate the Brownian diffusion effect on electrical mobility classification in the EMS to give a better understanding on the operation of the analyzer. Calculations were performed for particle size range from 1 nm to 500 nm. The particles were assumed to be fly ash particles. Their density and dielectric constant were 700 kg/m^3 and 3.0, respectively [29]. A uniformly distributed particle concentration at the entrance, a constant electrometer ring width (19 mm), a given ring separation (1 mm) and a fixed number of electrometer rings (22 rings) were as-

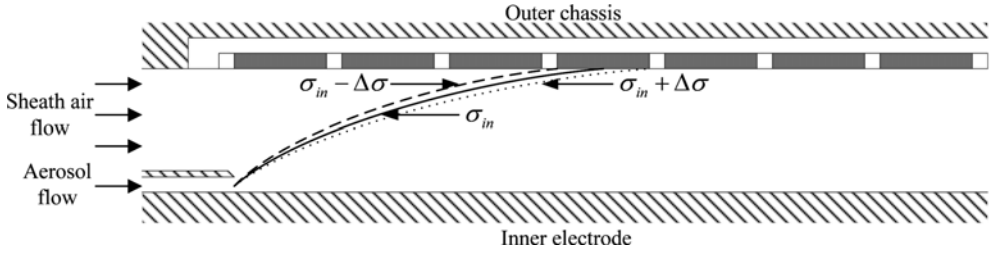

Fig. 3. Schematic diagram of diffusing particle trajectory in the EMS.

sumed. The parameters and operating conditions used are shown in Table 2. Air density and viscosity are 1.225 kg/m^3 and 1.7894×10^{-5} kg/m/s, respectively. A temperature of 294 K is used. In this study, the flow conditions inside the EMS were assumed to be steady, incompressible and laminar. The electric field distribution inside the analyzer was also assumed to be uniform in the axial direction. These calculations were carried out at varying aerosol flow rates between 2.5 to 5.0 *l*/min and sheath air flow rate was set at 35.0 *l*/min, corresponding to the Reynolds numbers in the range of 661 and 705. The flow regimes were clearly laminar. An operating pressure was varied in the range between 0.25 and 1 bar. The inner electrode voltage was varied from 2 to 4 kV. The dimensionless parameter $\overline{D}/\overline{E}$ and the diffusing particle trajectories were calculated by using Eqs. (18), (19) and (25), respectively, with MATLAB. The flow chart of the analytical model used in this study is shown in Fig. 4.

Table 2. Model parameter and operating condition values

Parameter and operating conditions	Values
Diameter of inner electrode, r_1 (mm)	25
Diameter of electrometer ring, r_2 (mm)	55
Length of analyzer, z (mm)	460
Applied voltage on the inner electrode, V (kV)	2, 4
Aerosol flow rate, Q_a (lpm)	2.5, 5.0
Sheath air flow rate, Q_{sh} (lpm)	35
Nature of flow	Laminar
Reynolds number	661-705
Operating temperature, T (K)	294
Operating pressure, P (atm)	0.25, 0.50, 0.75, 1
Gas density, (kg/m^3)	1.225
Gas viscosity, μ (kg/m/s)	1.7894×10^{-5}
Electrical mobility of ion, Z_i m^2/V/s	1.4×10^{-4}
Particle size range, d_p (nm)	1-500
Particle density, (kg/m^3)	700
Particle shape	Spherical
Particle dielectric constant	3.0

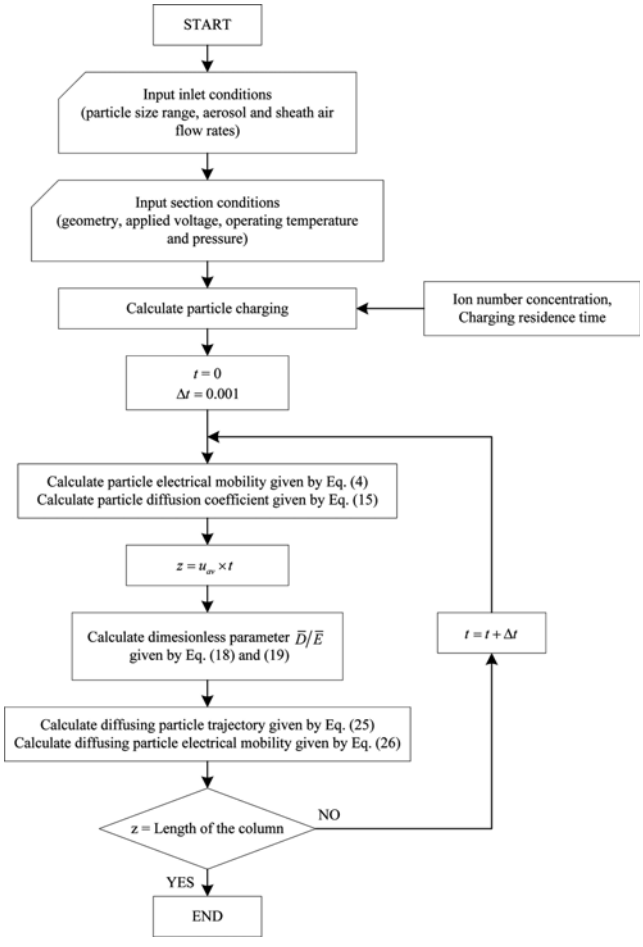

Fig. 4. Flow chart of the analytical model used in this study.

RESULTS AND DISCUSSION

In this Section, theoretical results of Brownian diffusion effect on nanometer aerosol classification in the EMS are discussed. The calculation of the dimensionless parameter $\overline{D}/\overline{E}$, and the particle trajectory and electrical mobility with and without Brownian diffusion effect were presented. Different conditions were studied in which the inner electrode voltage, aerosol flow rate, operating pressure, and particle diameter were varied.

Fig. 5 shows variation of the dimensionless parameter $\overline{D}/\overline{E}$ at each electrometer ring with operating pressure. $\overline{D}/\overline{E}$ was found to be on the order of 10^{-3} to 10^{-6}. It should be noted that the Brownian diffusion effect becomes important when $\overline{D}/\overline{E}$ is larger than 10^{-5} [16]. It can be seen in the plot that values of the dimensionless parameter $\overline{D}/\overline{E}$ decreased with increasing electrometer ring number. This was anticipated because an increase in the number of the electrometer ring referred to an increase in particle size. For a given ring number, the value of $\overline{D}/\overline{E}$ was influenced by operating pressure. A decrease in pressure resulted in a decrease in $\overline{D}/\overline{E}$. This may be attributed to the fact that reduction in operating pressure of the analyzer would tend to increase diffusion coefficient and mean free

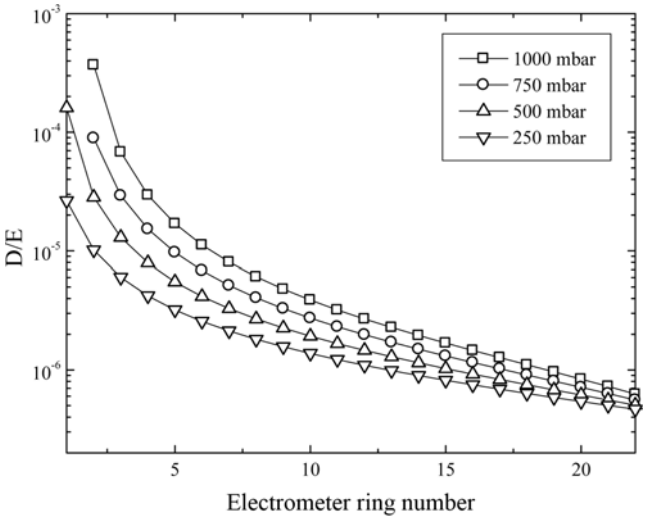

Fig. 5. Variation of dimensionless parameter $\overline{D}/\overline{E}$ at each electrometer ring of the EMS with operating pressure (2.0 kV inner electrode voltage, 2.5 *l*/min aerosol flow, and 35.0 *l*/min sheath air flow).

path of the particles, leading to an increase of electrical mobility resolution. It was also observed that there was no value of $\overline{D}/\overline{E}$ at electrometer ring number 1 for operating pressures of 0.75 and 1 bar. This is because there is no particle deposited on this electrometer ring at these operating pressures. Fig. 6 shows the variation of the dimensionless parameter $\overline{D}/\overline{E}$ at each electrometer ring with inner electrode voltage and aerosol flow rate. The inner electrode voltage was considered for 2 and 4 kV and aerosol flow rate was considered for 2.5 and 5.0 *l*/min, while the sheath air flow and operating pressure were set at 35.0 *l*/min, and 250 mbar, respectively. It was shown that short residence time (high aerosol flow rate), and low inner electrode voltage gave rise to minimum values of $\overline{D}/\overline{E}$ for each electrometer ring within the analyzer. It was implied that particle Brownian diffusion inside the EMS increased with decreasing flow rate and increasing inner electrode voltage. The particle diffusion coefficient is a function of the particle electrical mobility and number of charge on the particle. An increase in the inner electrode

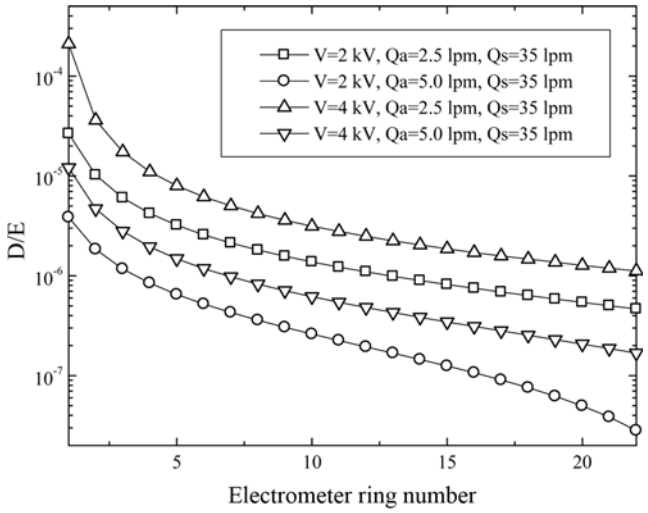

Fig. 6. Variation of dimensionless parameter $\overline{D}/\overline{E}$ at each electrometer ring of the EMS with inner electrode voltage and aerosol flow rate (35.0 *l*/min sheath air flow, and 250 mbar operating pressure).

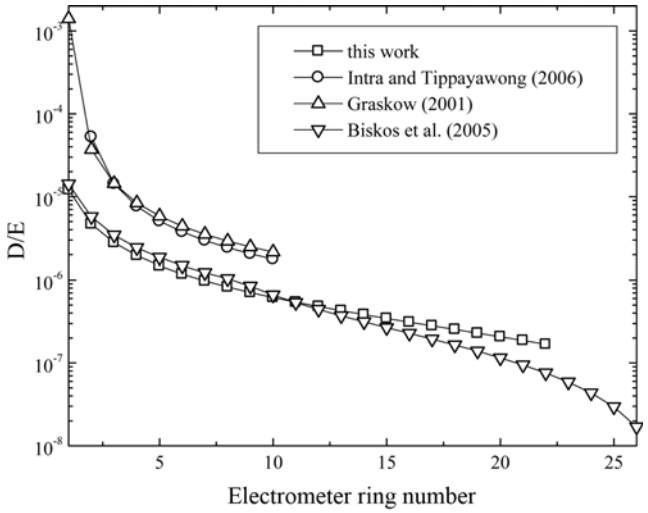

Fig. 7. Comparison of the dimensionless parameter $\overline{D}/\overline{E}$ between the present EMS and the existing EMS (4.0 kV inner electrode voltage, 5.0 *l*/min aerosol flow, 35.0 *l*/min sheath air flow, and 250 mbar operating pressure).

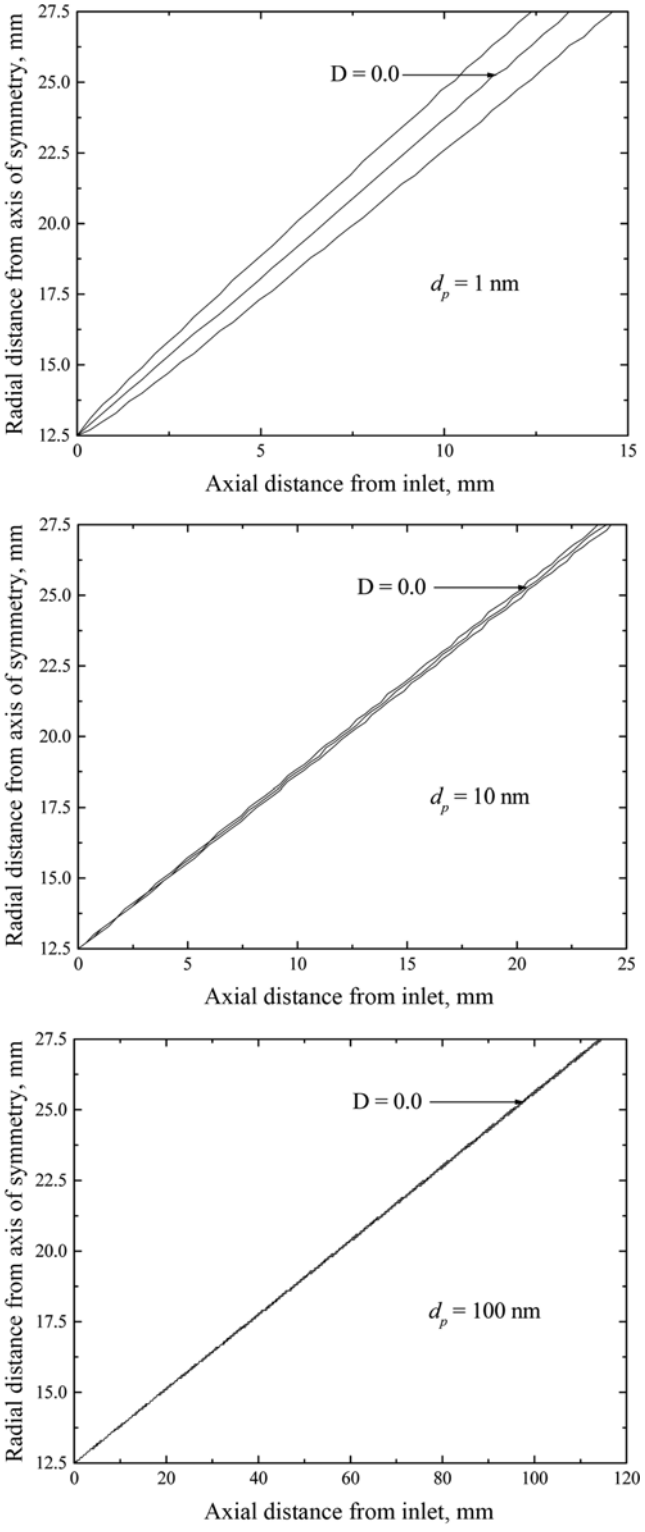

Fig. 8. Effect of Brownian diffusion on the central particle trajectory in the EMS for the particle diameters of 1, 10, and 100 nm.

voltage resulted in an increase of the electrical mobility of particles, corresponding to the particle size. Higher aerosol flow rate, hence, shorter residence time appeared to suppress Brownian diffusion effect on particle motion.

A comparison of the dimensionless parameter $\overline{D}/\overline{E}$ between several MCDMAs is shown in Fig. 7. The operating conditions of these analyzers were: 4.0 kV inner electrode voltage, 5.0 *l*/min aerosol flow, 35.0 *l*/min sheath air flow, and 250 mbar operating pressure. The values of $\overline{D}/\overline{E}$ are between 10^{-3} and 10^{-8}. It was shown that $\overline{D}/\overline{E}$ at each electrometer ring of the present EMS was slightly less than the analyzers by Graskow [11] and Intra and Tippayawong [13,14] and similar with that used by Biskos et al. [12]. The most diffusive particles were detected near the entrance of the analyzer column. Fig. 8 shows the particle trajectories in the analyzer column with and without taking into account the Brownian diffusion effect for particle diameters of 1, 10, and 100 nm. D=0.0 indicated the non-diffusing trajectory. Lines on either side of the central trajectory indicated the diffusing trajectories. It was shown that finer particles were found to exhibit higher Brownian diffusive motion than the larger particles. It is apparent that Brownian diffusion significantly affects particle trajectories when the diameter is smaller than 10 nm.

The difference in the spatial distribution of the electrical mobility inside the EMS is shown in Fig. 9. It can be seen that an increase in axial distance away from the inlet resulted in a marked discrepancy in the electrical mobility with and without the Brownian diffusion effect. It was clear that Brownian diffusion effect was significant in the EMS. If the Brownian diffusion effect was neglected, a significant error would be produced. Fig. 10 shows the variation of the diffusing particle electrical mobility with axial distance at different operating applied voltages, aerosol flow rates, and pressures. Results were evaluated for 2-4 kV, 2.5-5.0 *l*/min, and 250-1,000 mbar, considering the Brownian diffusion effect. The higher aerosol flow rate, hence the shorter residence time, gave rise to higher electrical mobility. Increase in inner electrode voltage resulted in a decrease in the electrical mobility along the analyzer column. At lower operating pressure, electrical mobility was slightly higher. It has been demonstrated here that an analytical model of the Brownian diffusion effect on nanometer aerosol classification was particularly useful in improving the resolution of the particle size distribution, the accuracy of electrical mobility classification, and particle loss due to Brownian diffusion.

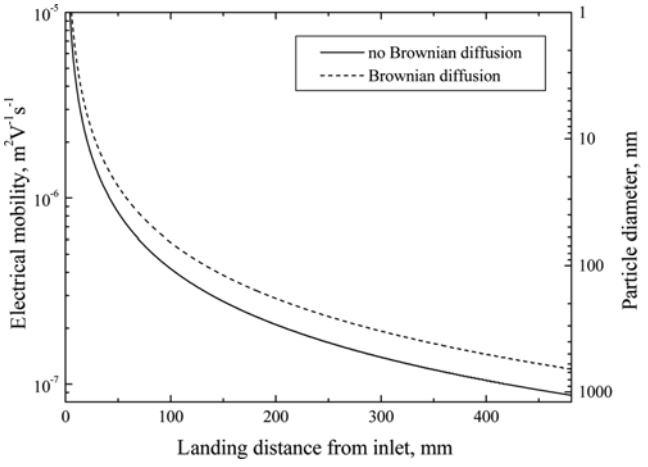

Fig. 9. Axial variation of the electrical mobility inside the EMS.

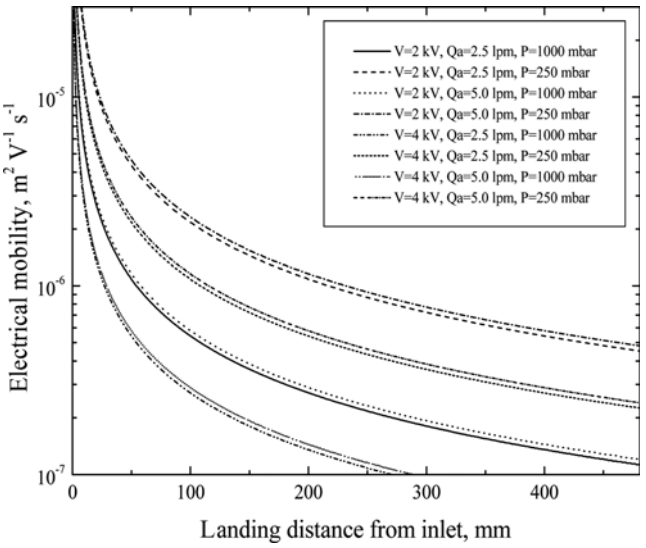

Fig. 10. Variation of the electrical mobility with axial distance at different operating applied voltage, aerosol flow rate, and pressure.

CONCLUSION

Investigation of the effect of Brownian diffusion of nanometer aerosol particles on the electrical mobility classification in the EMS developed at Chiang Mai University has been carried out. It was shown that the Brownian diffusion of particles increased with a reduction in particle size and flow rates, and an increase in operating pressure and inner electrode voltage. The Brownian diffusion effect becomes significant when the dimensionless parameter $\overline{D}/\overline{E}$ is larger than 10^{-5}. The value of $\overline{D}/\overline{E}$ in the present EMS was comparable to previously developed analyzers. Due to the effect of Brownian diffusion, broadening of the particle trajectories in the analyzer column was evident. Smaller particles appeared to be adversely affected in higher degree than the larger particles, especially particles with diameter smaller than 10 nm.

ACKNOWLEDGMENT

This work was supported by the National Electronic and Computer Technology Center, National Science and Technology Development Agency, Thailand.

NOMENCLATURE

C_c : Cunningham slip correction factor [-]
d_p : particle diameter [m]
D : particle diffusion coefficient [m^2/s]
$\overline{D}$: dimensionless parameter [-]
D_{atm} : particle diffusion coefficient at atmospheric pressure [m^2/s]
e : value of elementary charge on an electron [C]
E : electric field strength [V/m]

$\overline{E}$: dimensionless parameter [-]
E_r : radial components of the electric field [V/m]
E_z : axial components of the electric field [V/m]
k : Boltzmann's constant [J/K]
n : particle number concentration [particles/m^3]
n_p : average number of elementary charges on the particle [-]
P : operating pressure [atm]
P_{atm} : reference pressure [atm]
Q_a : aerosol flow rate [*l*/min]
Q_{sh} : sheath air flow rate [*l*/min]
Q_t : total flow rate [*l*/min]
r : radial coordinate [m]
r_1 : inner radius of the annulus [m]
r_2 : outer radius of the annulus [m]
r_{diff} : radial position for diffusive particles [m]
r_{in} : radial position at the particle enters the analyzer [m]
t : mean aerosol residence time [s]
T : absolute temperature [K]
u : flow velocity [m/s]
$\overline{u}(\overline{r})$: dimensionless parameter [-]
u_{av} : average flow velocity [m/s]
u_r : radial components of the flow velocity [m/s]
u_z : axial components of the flow velocity [m/s]
V : potential [V]
z : axial position [m]
Z_{patm} : particle electrical mobility at atmospheric pressure [m^2/V·s]
$Z_{p,\,diff}$: diffusing particle electrical mobility [m^2/V·s]

Greek Letters

μ : air viscosity [Pa·s]
σ : standard deviation of particle trajectory [-]

Subscripts

a : aerosol
r : radial direction
sh : sheath air
z : axial direction

REFERENCES

1. P. Intra and N. Tippayawong, *Songklanakarin J. Sci. Technol.*, **30**(2), 243 (2008).
2. B. Y. H. Liu and D. Y. H. Pui, *J. Colloid Inter. Sci.*, **47**, 155 (1974).
3. E. O. Knutson and K. T. Whitby, *J. Aerosol Sci.*, **6**, 443 (1975).
4. P. Intra and N. Tippayawong, *Mj. Int. J. Sci. Tech.*, **1**, 120 (2007).
5. E. A. Yunker, *Terr. Magn. Atmos. Electr.*, **45**, 127 (1940).
6. H. F. Tammet, A. F. Jakobson and J. J. Salm, *Acta Comm. Univ. Tartu 320*, 48 (1973).
7. A. Mirme, M. Noppel, I. Peil, J. Salm, E. Tamm and H. Tammet, *In 11th Int. Conf. on Atmospheric Aerosols, Condensation and Ice Nuclei*, Budapest, 2, 155 (1984).
8. R. Matisen, F. Miller, H. Tammet and J. Salm, *Acta Comm. Univ. Tartu 947*, 60 (1992).
9. A. Mirme, *Electric aerosol spectrometry*, Ph.D. Thesis, University of Tartuensis, Tartu, Estonia (1994).
10. H. Tammet, A. Mirme and E. Tamm, *Atmos. Res.*, **62**, 315 (2002).
11. B. R. Graskow, *Design and development of a fast aerosol size spectrometer*, Ph.D. Thesis, University of Cambridge, UK (2001).
12. G. Biskos, K. Reavell and N. Collings, *Aerosol Sci. Tech.*, **39**, 527 (2005).
13. P. Intra and N. Tippayawong, *Int. Conf. on Technology and Innovation for Sustainable Development*, Khon Kaen, Thailand, 25-27 January (2006).
14. P. Intra and N. Tippayawong, *J. Aerosol Res.*, **21**(4), 329 (2006).
15. J. H. Kim, *Korean J. Chem. Eng.*, **25**, 377 (2008).
16. Y. Kousaka, K. Okuyama, M. Adachi and T. Mimura, *J. Chem. Eng. Japan*, **19**(5), 401 (1986).
17. J. Zeleny, *Phys. Rev.*, **34**, 310 (1929).
18. H. Tammet, *The aspiration method for the determination of atmospheric ion-spectra*, IPST for NSF, Jerusalem (1970).
19. M. Stolzenburg, *An ultrafine aerosol size distribution measuring system*, PhD Thesis, University of Minnesota (1988).
20. J. Salm, *Aerosol Sci. Tech.*, **32**, 602 (2000).
21. C. Hagwood, Y. Sivathanu and G. Mulholland, *Aerosol Sci. Tech.*, **30**, 40 (1999).
22. P. Intra and N. Tippayawong, *Chiang Mai Univ. J.*, **6**, 313 (2007).
23. H. Tammet, *J. Aerosol Sci.*, **26**, 459 (1995).
24. Z. Li and H. Wang, *Phys. Rev. E.*, **68**, 061206 (2003).
25. S. D. Shandakov, A. G. Nasibulin and E. I. Kauppinen, *J. Aerosol Sci.*, **36**, 1125 (2005).
26. T. Seto, T. Nakamoto, K. Okuyama, M. Adachi, Y. Kuga and K. Takeuchi, *J. Aerosol Sci.*, **28**, 193 (1997).
27. M. Alonso and Y. Kousaka, *J. Aerosol Sci.*, **27**, 1201 (1996).
28. M. Alonso, Y. Kousaka, T. Hashimoto and N. Hashimoto, *J. Aerosol Sci.*, **29**, 985 (1998).
29. W. C. Hinds, *Aerosol technology*, John Wiley & Sons, New York (1999).